Bachelor Thesis

Computation of the static force in 1+1 dimensional SU(2) Yang-Mills theory

Michael Eichberg

September 2019

Institut für theoretische Physik
Goethe Universität
Franfurt am Main

1. Supervisor:
Prof. Dr. Marc Wagner
Insitut für theoretische Physik
Goethe Universität
Frankfurt a. M.

2. Supervisor:
Prof. Dr. Owe Philipsen
Insitut für theoretische Physik
Goethe Universität
Frankfurt a. M.

Erklärung nach § 30 (12) Ordnung für den Bachelor- und dem Masterstudiengang

Hiermit erkläre ich, dass ich die Arbeit selbstständig und ohne Benutzung anderer als der angegebenen Quellen und Hilfsmittel verfasst habe. Alle Stellen der Arbeit, die wörtlich oder sinngemäß aus Veröffentlichungen oder aus anderen fremden Texten entnommen wurden, sind von mir als solche kenntlich gemacht worden. Ferner erkläre ich, dass die Arbeit nicht - auch nicht auszugsweise - für eine andere Prüfung verwendet wurde.

Frankfurt, den

Abstract

The straight-forward way to compute a force is to take the derivative of the corresponding potential. This thesis explores an alternative way to compute the static force in $1+1$ dimensional $SU(2)$ Yang-Mills theory. The force is computed using a chromo-electric field correlator. Renormalization of colour fields, which is necessary in $3+1$ dimensions, is discussed and explored numerically. The static force computed from the slope of the static potential does not need renormalization and can be compared with the bare and renormalized force computed from the chromo-electric field. A known renormalization for $3+1$ dimensions is the Huntley-Michael method. For $1+1$ dimensions it will be interesting to see, if renormalization is necessary and if one can apply the Huntley-Michael method.

Contents

1 Introduction

Particles in quantum field theory are represented by fields which show certain transformation behaviour. Gauge transformations can be represented by group elements of $U(1)$ or $SU(N)$. The Lagrange density describes the dynamics of a theory. Conserved quantities in nature are contained in the Lagrangian as symmetries. Quantum chromodynamics is an example for a gauge theory with $SU(3)$-colour symmetry, which describes the dynamics of strongly interacting fermions and gauge bosons. Yang-Mills theory is a $SU(N)$ gauge theory and expresses gauge field dynamics of non-abelian fields with static quarks. These gauge fields are able to interact among themselves [1, 2].

In lattice gauge theory, discretization of Yang-Mills theory introduces gauge fields as link variables, elements of the gauge group. These link variables can be used to construct gauge invariant observables. Physical quantities can be extracted from correlators of observables. The Wilson loop is an observable which correlates a quark-antiquark-state with spatial size r with itself over temporal extension t. Writing the Wilson loop correlator in an expansion of eigenstates, the lowest state dominates in the limit $t \to \infty$ and describes the static quark-antiquark pair. The energy of the lowest state is therefore defined as the static quark potential (see section 3.3 in reference [3]).

By definition, the static force can be extracted from the results for the potential as the spatial derivative. An alternative way proposed very recently to extract the force directly from the lattice is to compute the ratio of a chromo-electric field correlator and a Wilson loop [4]. The chromo-electric field is inserted at the quark line of a Wilson loop. On the lattice, this field is constructed from plaquettes, which contain the lattice field strength tensor.

Colour field correlators are important tools to explore certain quantities in lattice QCD, examples can be found in references [5, 6]. In $3 + 1$ dimensions, colour fields are affected by self-energy contributions, which leads to renormalization becoming necessary [7]. One way to renormalize is the Huntley-Michael method. It is expected to remove self-energy contributions up to order $\mathcal{O}(\hat{g}^2 a^4)$ in perturbation theory. For computations using colour fields, reference values

which do not need renormalization are often unknown. For the force computed using a chromo-electric field, the slope of the potential is a known reference. The necessity of renormalization in $1 + 1$ dimensions can be explored by comparing the results of the force from the bare and renormalized fields with the force given by the slope of the potential [8].

Chapter 2 in this thesis introduces a lattice formulation for $SU(2)$ Yang-Mills theory. Steps to extract the static potential will be discussed, followed by the static force. The main part of this discussion will be the replacement of the spatial derivative in the definition of the force with a chromo-electric field, as existing references do not provide a detailed derivation. Afterwards, the Huntley-Michael method will be introduced. Results for the potential and the force are given in chapter 3, which also presents the lattice setup and discusses numerical methods. Chapter 4 gives a summary of the findings of this thesis with an outlook for possible next steps.

2 Theoretical basics

2.1 Lattice formulation for Yang-Mills theory

Constructing a formulation of Yang-Mills theory in $1+1$ dimensions is equivalent to $3+1$ dimensions. In $3+1$ dimensions, the coupling is dimensionless. This is not the case in $1+1$ dimensions. The lattice counterpart of the coupling g in $1+1$ dimensions will be $\hat{g} = g \cdot a$ with lattice spacing a.

The gauge fields are represented by group elements of $SU(2)$ and for $U, \Omega \in SU(2)$ at lattice point $n \in \Lambda$ the gauge transformation is given by [3]:

$$U_\mu(n) \to U'_\mu(n) = \Omega(n) U_\mu \Omega^\dagger(n+\hat{\mu}) \tag{2.1}$$

and one defines

$$U_\mu(n) = exp(i\hat{g} a A_\mu(n)) \tag{2.2}$$

The transformation behaviour in equation (2.1) suggests to construct a gauge invariant object from the trace of a closed loop of these link variables, as transformation matrices $\Omega, \Omega^\dagger$ of neighbouring links result in unit matrices. The smallest non-trivial closed loop is the plaquette $U_{\mu\nu}$, the indices indicate the direction of the plaquette.

Using the plaquette and cyclicity of the trace, the gauge invariant Wilson action is [3]:

$$\begin{aligned} S_G[U] &= \frac{\hat{\beta}}{N} \sum_{n\in\Lambda} \sum_{\mu<\nu} Re\, Tr\left(\mathbb{1} - U_{\mu\nu}(n)\right) \\ &= \frac{a^d}{2g^2} \sum_{n\in\Lambda} Tr\left(F_{\mu\nu}(n)^2\right) + \mathcal{O}(a^2) \end{aligned} \tag{2.3}$$

with $N = 2, d = 2$ and inverse lattice-coupling $\hat{\beta} = \frac{2N}{\hat{g}^2}$. In equation (2.3) one can see, that in $1+1$ dimensions the coupling g has mass dimension 1, whereas $\hat{\beta}$ is kept dimensionless.

For the relation between the plaquette and the field strength tensor in equation (2.3) one finds

$$\begin{aligned} U_{\mu\nu}(n) &= \exp\left(i\hat{g}a^2 F_{\mu\nu}(n) + \mathcal{O}(a^3)\right) \\ &= \mathbb{1} + i\hat{g}a^2 F_{\mu\nu}(n) - \hat{g}^2 a^4 F_{\mu\nu}(n)^2 + \mathcal{O}(a^6) \end{aligned} \tag{2.4}$$

The field strength tensor $F_{\mu\nu}$ has real entries only. Therefore, terms of order $\mathcal{O}(a^2)$ in the action vanish after taking the real part of the trace.

Using equation (2.3) for the gauge field action on the lattice, the expectation value of an observable $\langle O \rangle$ is defined using the euclidean path integral over group elements U:

$$\langle O \rangle := \frac{1}{Z} \int \mathcal{D}U \, O[U] \, e^{-S_G[U]}, \qquad Z = \int \mathcal{D}U \, e^{-S_G[U]} \tag{2.5}$$

The Haar measure $\mathcal{D}U$ and the observable O have to be invariant, as it is shown in section 3.2 reference [3].

2.2 Wilson loops and the static quark potential

In the following, the notation and argumentation in section 3.3 of reference [3] are used to discuss the Wilson loop. One starts with taking the trace of a closed loop $\mathcal{W}$ of link variables, which according to equation (2.1) leads to a gauge invariant observable. Separating the path into a so-called Wilson line $S(\mathbf{m}, \mathbf{n}, N_t)$ in spatial direction, a temporal line $T(\mathbf{n}, N_t)^\dagger$ and closing the loop with $S(\mathbf{m}, \mathbf{n}, 0)^\dagger$ and $T(\mathbf{m}, N_t)$, one has constructed a Wilson loop [3].

$$\begin{aligned} Tr\, W &= \frac{1}{N} \mathcal{P} \prod_{(\mu,n)\in\mathcal{W}} U_\mu(n) \\ &= \frac{1}{N} S(\mathbf{m}, \mathbf{n}, N_t) T(\mathbf{n}, N_t)^\dagger S(\mathbf{n}, \mathbf{m}, 0)^\dagger T(\mathbf{m}, N_t) \end{aligned} \tag{2.6}$$

With path ordering operator $\mathcal{P}$. To see, how the Wilson loop behaves as a function of temporal and spatial extensions ($T/a = N_t, r/a = N_r$), it is convenient to consider temporal gauge. Section 3.3 in reference [3] argues fixing the gauge will not change the outcome of the results, as the Wilson loop is a gauge-invariant observable. In temporal gauge, time-components of the 4-vector potential A_μ in a Wilson loop are set to 0, leading to

$$U_0(n) = exp\,(i\hat{g}aA_0(n)) = \mathbb{1}, \qquad n \in \Lambda \tag{2.7}$$

Using this the Wilson loop expectation value can be rewritten as

$$\begin{aligned} \langle Tr\, W\rangle &= \langle Tr\, W\rangle_{temp} \\ &= \frac{1}{N}\langle Tr\left(S(\mathbf{m},\mathbf{n},N_t)S(\mathbf{m},\mathbf{n},0)^\dagger\right)\rangle_{temp} \\ &= \frac{1}{N}\langle S_{ab}(\mathbf{m},\mathbf{n},n_t)S_{ba}(\mathbf{m},\mathbf{n},0)^\dagger\rangle_{temp} \end{aligned} \tag{2.8}$$

In equation (2.8) one will recognize the Wilson loop as the correlator between two Wilson lines. In the limit of infinitely large temporal lattice size, one can expand (2.8) in terms of eigenstates of the system:

$$\begin{aligned} \langle S_{ab}(\mathbf{m},\mathbf{n},n_t)S_{ba}(\mathbf{m},\mathbf{n},0)^\dagger\rangle_{temp} &= \sum_k \langle 0|\hat{S}_{ab}(\mathbf{m},\mathbf{n})|k\rangle \\ &\quad \times\langle k|\hat{S}_{ba}(\mathbf{m},\mathbf{n})^\dagger|0\rangle\, e^{-TE_k} \\ &= \sum_k |a_k|^2\, e^{-TE_k} \end{aligned} \tag{2.9}$$

with sum over all states $|k\rangle$ which have a non-vanishing overlap with $\hat{S}_{ab}(\mathbf{m},\mathbf{n})|0\rangle$ and corresponding energy E_k. Reference [3] argues in section 3.3 and discusses in chapter 5 in detail, that the Wilson lines express a quark-antiquark pair in the static limit. The spatial positions of the quark and antiquark are at $\mathbf{m},\mathbf{n}$ and one defines the static quark potential as the energy of the lowest state, E_1.

With energy gap ΔE between E_1 and the next state, $\langle Tr\, W\rangle$ can be expressed in the limit $T \to \infty$

$$\lim_{T\to\infty}\langle Tr\, W\rangle \propto e^{-TE_1}\left(1 + \mathcal{O}\left(e^{-T\Delta E}\right)\right) \tag{2.10}$$

Higher states are exponentially suppressed and E_1 is identified as the static quark potential [3]. The potential can be written as

$$\begin{aligned} V(r) &= -\lim_{T\to\infty} \frac{1}{T} \ln\langle Tr\, W\rangle \\ &= -\lim_{T\to\infty} \partial_T \ln\langle Tr\, W\rangle \\ &= -\lim_{T\to\infty} \lim_{a\to 0} \frac{1}{a}\, ln \left(\frac{\langle Tr\, W(r,T)\rangle}{\langle Tr\, W(r,T+a)\rangle} \right) \end{aligned} \tag{2.11}$$

The equivalence between the expressions in equation (2.11) can be seen when considering the linear behaviour of $\ln\langle W\rangle$ for $T \to \infty$.

The static potential in $1+1$ dimensions is discussed in reference [9] and found to be linear. It was argued, that in axial gauge $A_1(x) = 0$, the field strength tensor in the Yang-Mills Lagrangian reduces to $F_{01}(x) = -F_{10}(x) = -\partial_1 A_0(x)$, which does no longer contain time derivatives. As a result, the only gluons contributing to the Wilson loop are so-called ladder, or potential gluons and do neither interact among themselves, nor propagate in time. The result, similarly to the abelian case, is found to be linear:

$$V(r) \propto r \tag{2.12}$$

2.3 Extracting the static force

The force can be computed from the spatial derivative of the potential.

$$\begin{aligned} F(r) &= \partial_r V(r) \\ &= -\lim_{T\to\infty} \frac{1}{T} \frac{\partial_r \langle Tr\, W\rangle}{\langle Tr\, W\rangle} \end{aligned} \tag{2.13}$$

In $1+1$ dimensions, the force is constant.

In reference [4] an alternative formula to compute the force in Minkowski space is given. The corresponding formula in euclidean space is:

$$F(r) = -\lim_{T\to\infty} i \frac{\langle E\rangle_W}{\langle Tr\, W\rangle} \tag{2.14}$$

where $\langle E \rangle_W$ is a Wilson loop in which a chromo-electric field was inserted:

$$\langle E(t) \rangle_W = \langle Tr\, \mathcal{P}\, \hat{g} E(R,t) \prod_{(\mu,n)\in\mathcal{W}} U_\mu(n) \rangle \tag{2.15}$$

The clover definition of the chromo-electric field on the lattice is:

$$\hat{g} a^2 E_i = \frac{1}{2i} \left(\Pi_{i0} - \Pi_{i0}^\dagger \right) \tag{2.16}$$

with

$$\Pi_{\mu\nu} = \frac{1}{4} \left(U_{\mu\nu} + U_{\nu-\mu} + U_{-\mu-\nu} + U_{-\nu\mu} \right) \tag{2.17}$$

where $U_{\mu\nu}$ depicts the plaquette. This is called the clover definition of E, as the plaquettes look like four-leaf clover. The equivalence between equation (2.16) and $E_i = F_{i0} = -F_{0i}$ can be shown by expanding the plaquette (equation (2.4)), taking the imaginary part and averaging over all equivalent expressions.

The following provides a detailed derivation of equation (2.14). To understand the equivalence between equations (2.13) and (2.14), one has to make a few considerations. The derivative of W with respect to r takes the form

$$\begin{aligned} Tr\, \partial_r W(r,T) &= Tr\, \partial_r\, \mathcal{P}\, exp\left(i\hat{g} \oint_{\mathcal{W}} dz_\mu A_\mu(z) \right) \\ &= Tr \lim_{a\to 0} \frac{1}{a} \left(\mathcal{P}\, e^{i\hat{g} \oint_{\mathcal{W}'} dz_\mu A_\mu(z)} - \mathcal{P}\, e^{i\hat{g} \oint_{\mathcal{W}} dz_\mu a_\mu(z)} \right) \\ &= Tr \lim_{a\to 0} \mathcal{P}\, \frac{W(r,T)}{a} \left(e^{i\hat{g} \oint_{\Delta\mathcal{W}} dz_\mu A_\mu(z)} - 1 \right) \end{aligned} \tag{2.18}$$

where the integrals going along the loop $\mathcal{W}$, $\mathcal{W}'$ representing the path ordered product of links. The contour $\mathcal{W}'$ is $\mathcal{W}$ with a change $r \to r + a$ of the spatial extension. $\Delta\mathcal{W}$ is a contour with spatial extension a, which, if inserted into $\mathcal{W}$ equals $\mathcal{W}'$. Equation (2.18) inserts temporal lines $T(r,T)^\dagger T(r,T) = \mathbb{1}$ and makes use of the cyclicity of the trace in order to factor out a Wilson loop (see figure 2.1).

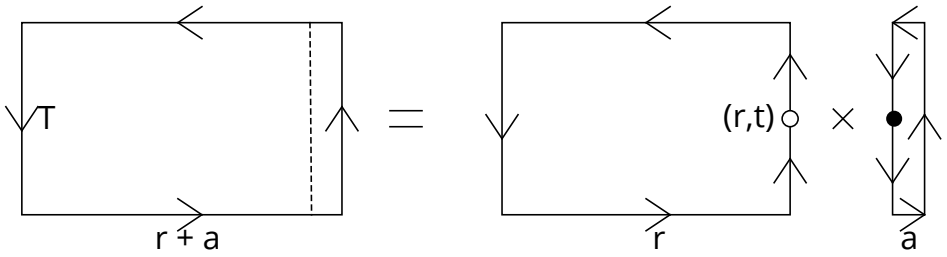

Figure 2.1: The Wilson loop of size $(r+a, T)$ can be written as a Wilson loop with spatial size r, where one inserts a loop at a point (r, t) on the quark line (hollow and filled circle). Using the cyclicity of the trace, this part can be factored out.

At the top of the contour $\Delta\mathcal{W}$, a $U_x^\dagger U_x = \mathbb{1}$ can be inserted in order to create a plaquette. Inserting unit matrices along the loop will not directly result in a chain of single plaquettes, as the links are path ordered. Nevertheless, the limit $a \to 0$ is implied in the following and the Baker-Campbell-Hausdorff formula can be applied. The goal is to merge all links along the contour in a single exponential, such that path ordering can be neglected. The Baker-Campbell-Hausdorff formula for exponential matrices with small parameter a is

$$exp(aX)exp(aY) \;=\; exp\left(aX + aY + \frac{a^2}{2}[X,Y] + \mathcal{O}(a^3)\right) \tag{2.19}$$

Applying this on the gauge links along $\Delta\mathcal{W}$ leads to:

$$\begin{aligned}
\mathcal{P}\, e^{i\hat{g}\oint_{\Delta\mathcal{W}} dz_\mu A_\mu(z)} &= ...U_x(n)U_t(n+\hat{x})U_x(n+\hat{t})^\dagger U_{xt}(n+\hat{t})U_t(n)^\dagger... \\
&= ... \cdot e^{i\hat{g}aA_x(n)} e^{i\hat{g}a^2F_{xt}(n+\hat{t})} \cdot ... \\
&= ... \cdot exp(i\hat{g}aA_x(n) + i\hat{g}a^2F_{xt}(n+\hat{t}) + i\hat{g}aA_t(n+\hat{x}) \\
&\quad -i\hat{g}A_x(n+\hat{t}) - i\hat{g}aA_t(n) \\
&\quad -\frac{\hat{g}^2a^2}{2}\left[A_x(n), A_t(n+\hat{x})\right] + \frac{\hat{g}^2a^2}{2}\left[A_x(n), A_x(n+\hat{t})\right] \\
&\quad +\frac{\hat{g}^2a^2}{2}\left[A_t(n), A_t(n)\right] + \frac{\hat{g}^2a^2}{2}\left[A_t(n+\hat{x}), A_x(n+\hat{t})\right] \\
&\quad +\frac{\hat{g}^2a^2}{2}\left[A_t(n+\hat{x}), A_t(n)\right] - \frac{\hat{g}^2a^2}{2}\left[A_x(n+\hat{t}), A_t(n)\right] \\
&\quad +\mathcal{O}(a^3)) \cdot ...
\end{aligned} \tag{2.20}$$

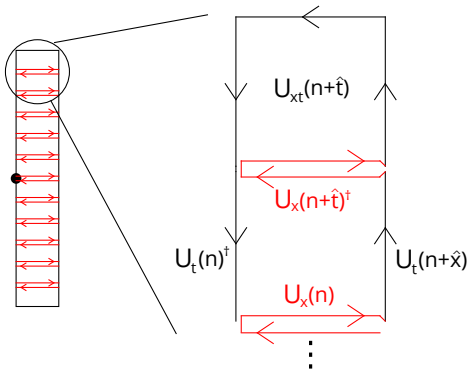

Figure 2.2: On the left side: $\Delta\mathcal{W}$ with inserted $U_x^\dagger U_x$. Right side: Close up look at the top part of $\Delta\mathcal{W}$. The plaquette $U_{xt}(n+\hat{t})$ is located at the upper end of the loop, $n+\hat{t} \mathrel{\hat{=}} (r, T-a)$. The black dot is located at (r,t), where $\Delta\mathcal{W}$ is placed in $\mathcal{W}$.

In the next step, $A_\mu(n+\hat{\nu})$ will be expressed using the derivative

$$A_\mu(n+\hat{\nu}) = A_\mu(n) + a\partial_\nu A_\mu(x)|_n + \mathcal{O}(a^2) \tag{2.21}$$

The commutators $[A_\mu(n+\hat{\rho}), A_\nu(n+\hat{\sigma})]$ are already $\mathcal{O}(a^2)$ and simply become $[A_\mu(n), A_\nu(n)] + \mathcal{O}(a^3)$. This leads to

$$\begin{aligned}
\mathcal{P}e^{i\hat{g}\oint_{\Delta\mathcal{W}} dz_\mu A_\mu(z)} &= ...exp(i\hat{g}a^2 F_{xt}(n+\hat{t}) \\
&\quad + i\hat{g}a^2\partial_x A_t(x)|_{x=n} - i\hat{g}a^2\partial_t A_x(x)|_{x=n} \\
&\quad - \frac{\hat{g}^2a^2}{2}[A_x(n), A_t(n)] + \frac{\hat{g}^2a^2}{2}[A_x(n), A_x(n)] \\
&\quad + \frac{\hat{g}^2a^2}{2}[A_x(n), A_t(n)] + \frac{\hat{g}^2a^2}{2}[A_t(n), A_x(n)] \\
&\quad + \frac{\hat{g}^2a^2}{2}[A_t(n), A_t(n)] - \frac{\hat{g}^2a^2}{2}[A_x(n), A_t(n)] \\
&\quad + \mathcal{O}(a^3)) \cdot ... \\
&= exp\left(i\hat{g}a^2\left(F_{xt}(n+\hat{t}) + F_{xt}(n) + \mathcal{O}(a)\right)\right) \cdot ...
\end{aligned} \tag{2.22}$$

Repeating this for all $T/a = N_t$ parts of $\Delta\mathcal{W}$ leads to

$$e^{i\hat{g}\oint_{\Delta\mathcal{W}} dz_\mu A_\mu(z)} = exp\left(i\hat{g}a^2\sum_{j=0}^{N_t-1}\left(F_{xt}(\mathbf{n}, j) + \mathcal{O}(a)\right)\right) \tag{2.23}$$

Now, all $A_\mu(n)$ are contained as the sum of the field strength tensors in one exponential.

The xt-element of the field strength tensor corresponds to the chromo-electric field E_x. Using $N_t = T/a$ in the lmit $a \to 0$, the sum can be rewritten as an integral. Plugging this into equation (2.18) yields:

$$\begin{aligned} \mathcal{P}e^{i\hat{g}\oint_{\Delta\mathcal{W}} dz_\mu A_\mu(z)} - 1 &= \mathcal{P}e^{i\hat{g}a\int_0^T dt(E(t)+\mathcal{O}(a))} - 1 \\ &= i\hat{g}a\int_0^T dt\,(E(t)+\mathcal{O}(a)) \quad (2.24) \\ \Rightarrow \lim_{a\to 0}\frac{W(r,T)}{a}\left(e^{i\hat{g}\oint_{\Delta\mathcal{W}} dz_\mu A_\mu(z)} - 1\right) &= W(r,T)\left(i\hat{g}\int_0^T dtE(t)\right) \quad (2.25) \end{aligned}$$

Expanding the exponential in equation (2.24) is only valid if the condition $aT \ll 1$ is fulfilled.

Using this result, the force in equation (2.13) can be rewritten as

$$\begin{aligned} F(r) &= -\lim_{T\to\infty}\frac{1}{T}\frac{\partial_r\langle Tr\,W\rangle}{\langle Tr\,W\rangle} \\ &= -\lim_{T\to\infty}\frac{i}{T}\frac{\langle Tr\,\mathcal{P}\int_0^T dt\hat{g}E(t)W\rangle}{\langle Tr\,W\rangle} \\ &= -\lim_{T\to\infty} i\frac{\langle Tr\,\mathcal{P}\,\hat{g}E(t)W\rangle}{\langle Tr\,W\rangle} \end{aligned} \quad (2.26)$$

where it was used that one can replace the integral $\int_0^T dt\hat{g}E(t)$ with $E(t)$, t far from 0 and ∞.

The correlator in the numerator in equation (2.26) is the definition of $\langle E\rangle_W$ in equation (2.14). Even though the correlators take traces over closed loops, which should be real, a factor of i is left. This can be explained with the lattice definition of the chromo-electric field. Equation (2.16) defines the chromo-electric field as the imaginary part of the first-order expansion of $U_\mu\nu(n)$ in a^2 (equation (2.4)). When looking at equation (2.14), inserting the definition of E from equation (2.16), the factor i cancels out and what is left are closed loops only.

$$ia^2\frac{\langle E\rangle_W}{\langle Tr\,W\rangle} = \frac{\langle\frac{1}{2}\left(\Pi_{xt} - \Pi_{xt}^\dagger\right)\rangle_W}{\langle Tr\,W\rangle} \quad (2.27)$$

with Π_{xt} as in equation (2.17).

2.4 Huntley-Michael procedure

In 3+1 dimensions, colour fields have to be renormalized. In the absence of exact renormalization procedures, one method is to apply a procedure formulated by A. Huntley and C. Michael [7]. It is a perturbative method and aims to eliminate self energies up to order $\mathcal{O}(g^2a^4)$. For colour fields, the force in equation (2.14) is multiplied with Z_E, defined as

$$Z_E{}^{-1} = \frac{\langle \bar{E} \rangle_W}{\langle W \rangle}, \tag{2.28}$$

$$\bar{E}_i = \frac{1}{2}\left(\Pi_{i0} + \Pi_{i0}^{\dagger}\right) \tag{2.29}$$

Colour field correlators are important tools in lattice gauge theories, a renormalization procedure is therefore of great interest. Examples for correlators using colour fields renormalized using this method in $3+1$ dimensions can be found in references [5, 6].

A detailed discussion about the need for renormalization in $1+1$ dimensional Yang-Mills theory and applicability of HM-renormalization is beyond the scope of this thesis and is therefore planned as a next step. If renormalization is not necessary, it will be seen in the continuum limit. Bare and renormalized results will not necessarily be identical, but can have different corrections in $\mathcal{O}(a^2)$ due to discretization. These corrections vanish in the continuum limit and the bare and renormalized results have to agree.

In the case of the static force, computing the slope of the static potential is a straight forward and physically well understood method. It is also a method for which renormalization is not necessary. This makes $\partial_r V(r)$ a possible candidate for a reference value and one can evaluate the force computed from the chromo-electric field by comparing it with $\partial_r V(r)$ [8].

3 Results

Random gauge field configurations are generated using a Monte-Carlo heatbath algorithm with Wilson action from equation (2.3). The program codes in C++ to generate random gauge field configurations and compute the correlators were existing in $3+1$ dimensions and had to be extended to also work in $1+1$ dimensions. A relation between $\hat{\beta}$ and the lattice spacing a is given as

$$\hat{\beta} = \frac{\beta}{a^2} \;\Leftrightarrow\; a = \sqrt{\frac{\beta}{\hat{\beta}}} \tag{3.1}$$

for a given β. The continuum limit is approached by increasing $\hat{\beta}$. Table (3.1) shows the setup. For $\hat{\beta} = 160$ the number of configurations is very low and should be considered in the evaluation.

In the absence of experimental data to find values for the lattice spacing a, the numerical results are given in terms of $\sqrt{\beta}$ as a reference scale or dimensionless ratios. For example, from Wilson loops, one gets $aV_{eff}(r)$ and $aV(r)$. In case of the force, the derivative of the potential and the lattice definition of E_x give $a^2F(r)$. Therefore, the ratio between results for equation (2.14) and the slope of the potential are a-independent and are used to compare the results.

Statistical errors are computed using the Jackknife method.

$\hat{\beta}$	a	$(L/a)^2$	# of configs
10	$\sqrt{\beta/10}$	100^2	10^4
40	$\sqrt{\beta/40}$	200^2	96
160	$\sqrt{\beta/160}$	400^2	11

Table 3.1: With the inverse lattice coupling $\hat{\beta}$ the lattice spacing is set. The lattice is quadratic and the length is chosen such that the physical size is the same for all $\hat{\beta}$. As the reference value β is unknown, a cannot be given in physical units.

3.1 Signal enhancement techniques

Commonly used steps to improve numerical data are smearing methods used to increase the overlap of a state with the vacuum. Spatial smearing, such as APE [10], is not applicable in $1+1$ dimensions.

As quantities like the static potential are defined as the logarithm of an expectation value, statistical errors in the limit $T \to \infty$ inflate quickly. In the case of Wilson loops, one can improve the results by applying HYP smearing methods [11]. The procedure affects the static potential by lowering the value of V_{eff} and therefore improving the signal-to-noise ratio. HYP smearing is applicable in $1+1$ dimension and will indeed lead to smaller errors.

3.2 Static potential

The first interesting results are the effective potentials $V_{\mathit{eff}}(r,T)$, using equation (2.11). One expects the effective potential to converge in time to a constant value, when higher states are suppressed exponentially. A suitable plateau is chosen, where V_{eff} has converged and errors are still small. The results for $\hat{\beta} = 40$ for various distances r/a is given in figure (3.1).

As the data appears to be constant in time, the plateaus for $V(r)$ start at the lowest T. This also implies that APE smearing is not needed.

After finding suitable plateaus in the effective potentials for each distance r, one can use the results to draw the static potential. As mentioned before, the potential is expected to be linearly rising. The static potentials for the different $\hat{\beta}$ of the set listed in table (3.1) are shown in figure (3.2).

For $r/a \geq 2$, the potential is linear, as expected. At $r/a < 2$, lattice discretization leads to a deviation from a linear behaviour.

The data shown in figure (3.2) depends on lattice spacing a, where a is different for each potential. To compare the potentials, one can draw the data in terms of $\sqrt{\beta}$. One can see, the potentials have similar traits, except a light shift from each other.

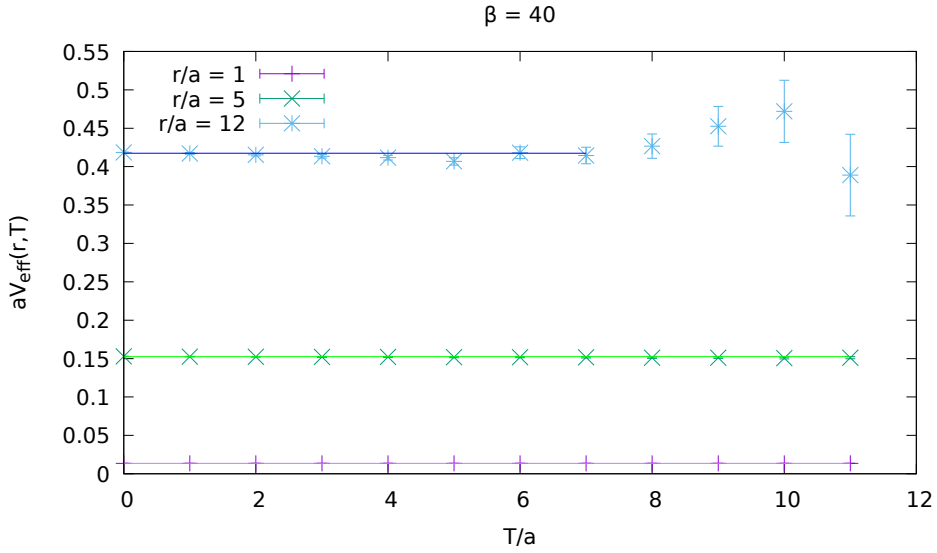

Figure 3.1: Effective potential for $\hat{\beta} = 40$ and $r/a = 1, 5, 12$ in terms of lattice spacing a. The chosen plateaus are shown as horizontal lines.

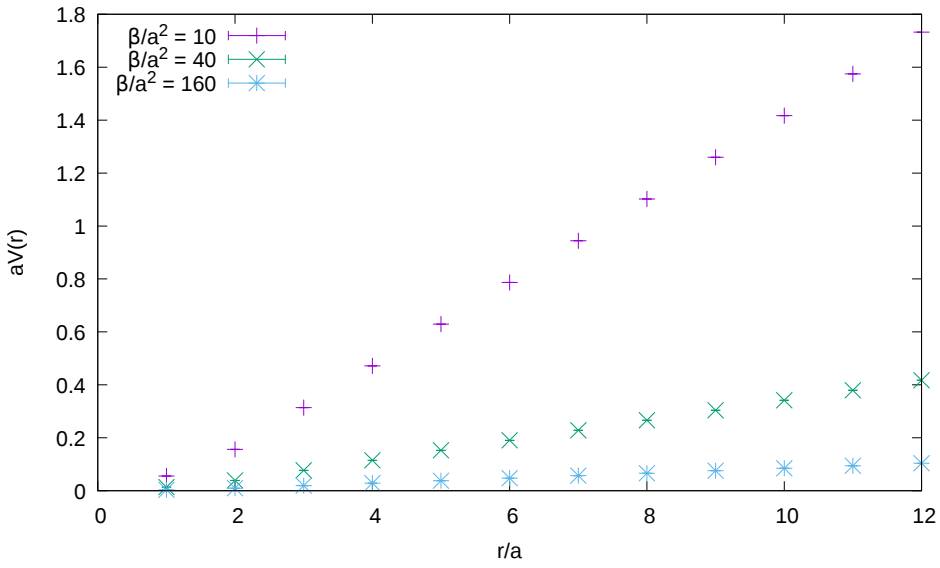

Figure 3.2: Static potential for $\hat{\beta} = 10, 40, 160$ in terms of a.

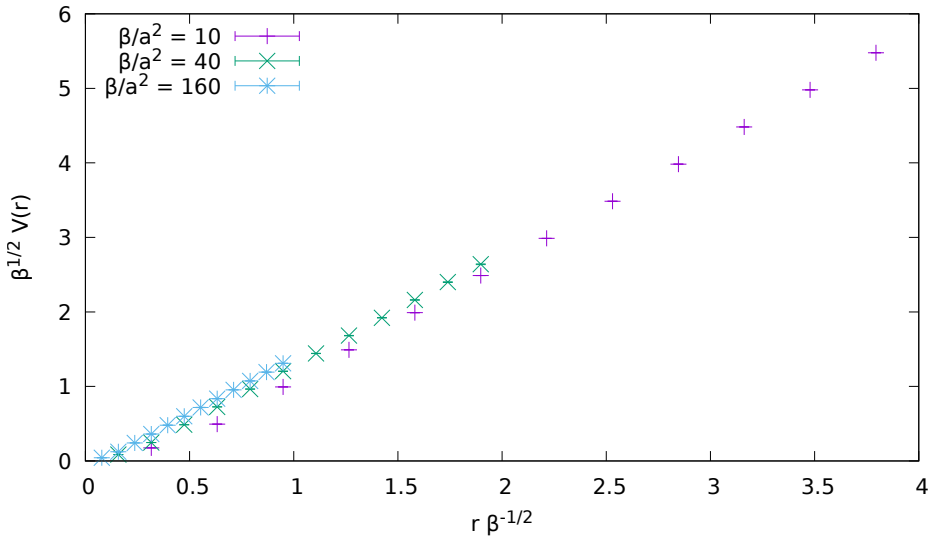

Figure 3.3: Static potential for $\hat{\beta} = 10, 40, 160$ in terms of $\sqrt{\beta}$.

3.3 Static force

Computing the force on the lattice will give $a\partial_r V(r) = a^2 F(r)$. For the alternative way, the definition of $\hat{g}a^2 E$ will also lead to $a^2 F(r)$. The ratio of $F(r)$ using equation (2.14) and the slope of the potential will not depend on a. It also gives the opportunity to evaluate the introduced formula in equation (2.14) by comparing it to $\partial_r V(r)$ from Wilson loops.

The results for the non-renormalized chromo-electric field will be compared with results renormalized using the Huntley-Michael procedure. Sizeable discretization errors errors are expected for $r/a \leq 2$.

Figure (3.4) shows the ratio between the force computed from the electric field correlator and the slope of the static potential for $\hat{\beta} = 10$, which corresponds to the largest lattice spacing a in the set. It shows small, but clear deviations between the force from the chromo-electric field and the reference $\partial_r V(r)$. The bare electric field has for all data points a smaller deviation than the electric field with Huntley-Michael renormalization.

In figure (3.5) and (3.6), $\hat{\beta}$ was raised by a factor of 4, which corresponds to the lattice spacing lowered by half. The points in figure (3.5) moved closer to the line at 1 and in figure (3.6), the errorbars are covering it. The deviation got visibly smaller for a smaller lattice spacing, with both, the bare and renormalized results, approaching the reference value $\partial_r V(r)$. This indicates that the alternative way to compute the force converges to the continuum result in the continuum limit.

A straight-forward assumption is, that the electric field in equation (2.16) has corrections in $\mathcal{O}(a^2)$. Figure (3.7) compares the bare and renormalized results for the force at different lattice spacings squared. In the scope of the statistical errors, a linear behaviour of the correction terms seems to be a good approximation. The linear fits for both data plots are consistent with the 1 in the continuum limit. The results renormalized with the Huntley-Michael renormalization factor have slightly larger corrections than the bare results. For the bare results this means, renormalization of the chromo-electric field seems not to be necessary.

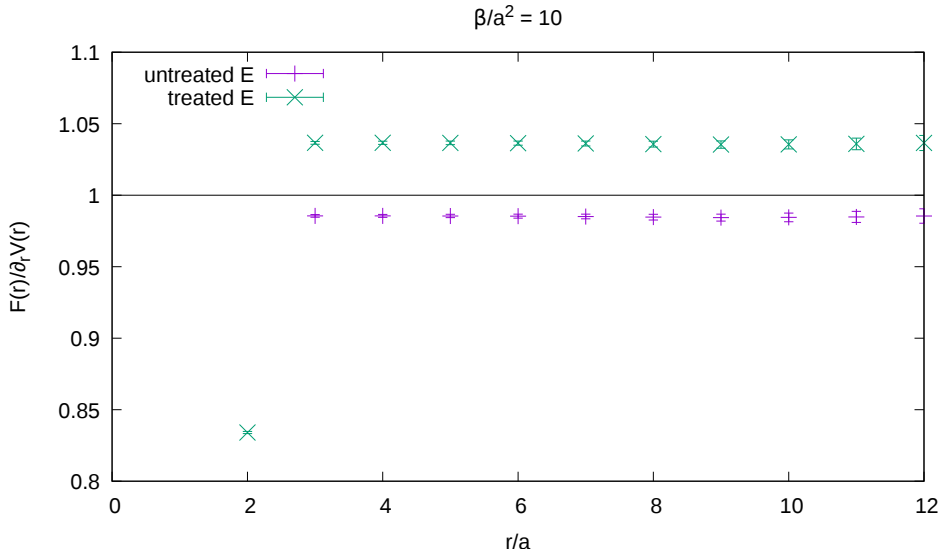

Figure 3.4: $F(r)/\partial_r V(r)$ with $F(r)$ computed from $\langle E\rangle_W/\langle Tr\, W\rangle$ in purple and $\langle E\rangle_W/\langle \bar{E}\rangle_W$ in green for $\hat{\beta} = 10$.

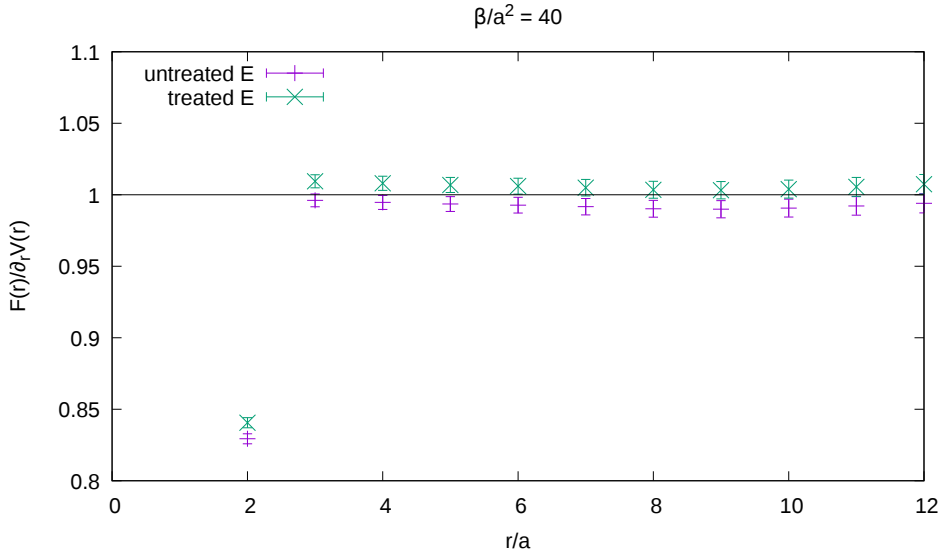

Figure 3.5: $F(r)/\partial_r V(r)$ as in figure (3.4) with $\hat{\beta} = 40$.

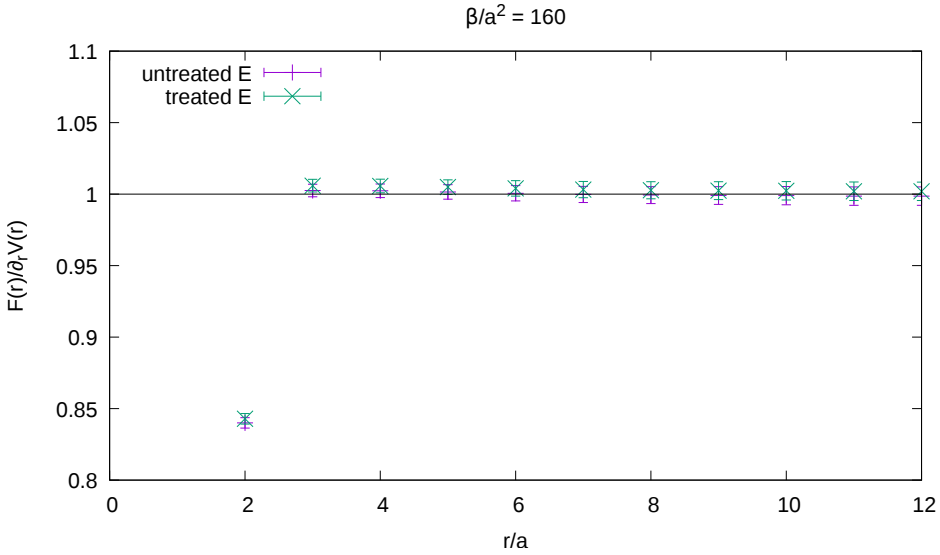

Figure 3.6: Results for the force at $\hat{\beta} = 160$.

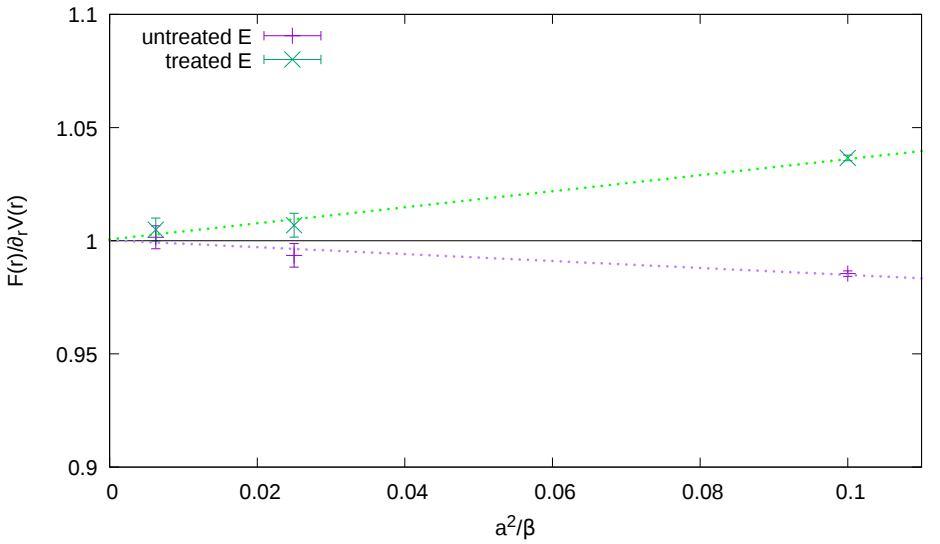

Figure 3.7: $F(r)/\partial_r V(r)$ at $r/a = 5$ for $\hat{\beta} = 10, 40, 160$.

4 Conclusions

4.1 Summary

This thesis explored an alternative way to compute the static force in $1+1$ dimensional $SU(2)$ Yang-Mills theory. The force is computed directly from the lattice using a chromo-electric field in a Wilson loop, which is shown to replace the spatial derivative of a Wilson loop correlator in the limit $T \to \infty$. As known from $3+1$ dimensions, discretization errors are large for $r/a \leq 2$. The continuum limit can be approached by increasing the inverse lattice-coupling $\hat{\beta}$.

As argued in reference [9], the $1+1$ dimensional static potential is linear and has a similar form as the abelian counterpart. The computations were able to reproduce the linear behaviour and the constant slope was determined. This slope was used as a reference for the static force, as this method does not need renormalization. Additionally, the technical procedure is straight-forward and theoretically well understood.

Colour fields in $3+1$ dimensions are affected by self-energy contributions and have to be renormalized. In this case, precise renormalization parameters are unknown. A perturbative procedure is the Huntley Michael method. This method was applied in $1+1$ dimensional Yang-Mills theory. With the slope of the static potential as a reference, the results renormalized using the HM-method are compared to the bare results with eyes on the continuum limit.

The setup consists of three ensembles with different lattice spacings. For the largest lattice spacing, both bare and renormalized results deviate from the reference, whereas the deviation appears to be larger for the results on which the HM-method was applied. With smaller lattice spacings, deviations become smaller in both cases. Both ways converge to the reference in the continuum limit, with bare results from below and renormalized ones from above. This indicates renormalization in $1+1$ dimensional Yang-Mills theory is not needed.

4.2 Outlook

In $1+1$ dimensional Yang-Mills theory, the only remaining colour field is the chromo-electric field. The results indicate, that the correlator of this field does not need a renormalization treatment, but has considerably large corrections at large lattice spacing. Applying the Huntley-Michael method leads to similar results, but the corrections have different signs. In both cases, the results converge to the reference result and are therefore a valid option.

Next steps include more statistics and a more detailed theoretical understanding of renormalization in $1+1$ dimensions. Furthermore, the case of $2+1$ dimensions can be explored. Additionally, a rigorous improvement of the correction terms will be useful.

Bibliography

[1] Michael E Peskin. *An introduction to quantum field theory*. CRC Press, 2018.

[2] Owe Philipsen. *Quantenfeldtheorie und das Standardmodell der Teilchenphysik: eine Einführung*. Springer-Verlag, 2018.

[3] Christof Gattringer and Christian Lang. *Quantum chromodynamics on the lattice: an introductory presentation*, volume 788. Springer Science & Business Media, 2010.

[4] Antonio Vairo. A low-energy determination of α_s at three loops. *EPJ Web Conf.*, 126:02031, 2016. [EPJ Web Conf.120,07004(2016)].

[5] Yoshiaki Koma and Miho Koma. Spin-dependent potentials from lattice QCD. *Nucl. Phys.*, **B769**:79–107, 2007.

[6] Gunnar S. Bali, Klaus Schilling, and Armin Wachter. Ab initio calculation of relativistic corrections to the static interquark potential. 1: SU(2) gauge theory. *Phys. Rev.*, **D55**:5309–5324, 1997.

[7] A. Huntley and Christopher Michael. Spin Spin and Spin - Orbit Potentials From Lattice Gauge Theory. *Nucl. Phys.*, **B286**:211–230, 1987.

[8] Viljamo Leino. Static force from lattice. *Poster at 37. Int. Symp. of LFT, Wuhan*, 2019.

[9] Antonio Pineda and Maximilian Stahlhofen. The QCD static potential in $D < 4$ dimensions at weak coupling. *Phys. Rev.*, **D81**:074026, 2010.

[10] M. Falcioni, M. L. Paciello, G. Parisi, and B. Taglienti. AGAIN ON SU(3) GLUEBALL MASS. *Nucl. Phys.*, **B251**:624–632, 1985.

[11] Anna Hasenfratz and Francesco Knechtli. Flavor symmetry and the static potential with hypercubic blocking. *Phys. Rev.*, **D64**:034504, 2001.